Accurate and precision Cosmology with redshift unknown gravitational wave sources

Suvodip Mukherjee,[1,*] Benjamin D. Wandelt,[2,3,4,†] Samaya M. Nissanke,[1,‡] and Alessandra Silvestri[5,§]

[1] *Gravitation Astroparticle Physics Amsterdam (GRAPPA), Anton Pannekoek Institute for Astronomy and Institute for High-Energy Physics, University of Amsterdam, Science Park 904, 1090 GL Amsterdam, The Netherlands*
[2] *Institut d'Astrophysique de Paris (IAP), UMR 7095, CNRS/UPMC Université Paris 6, Sorbonne Universités, 98 bis boulevard Arago, F-75014 Paris, France*
[3] *Institut Lagrange de Paris (ILP), Sorbonne Universités, 98 bis Boulevard Arago, 75014 Paris, France*
[4] *Center for Computational Astrophysics, Flatiron Institute, 162 5th Avenue, New York, NY 10010, USA*
[5] *Institute Lorentz, Leiden University, PO Box 9506, Leiden 2300 RA, The Netherlands*

(Dated: July 8, 2020)

Gravitational waves can provide an accurate measurement of the luminosity distance to the source, but cannot provide the source redshift unless the degeneracy between mass and redshift can be broken. This makes it essential to infer the redshift of the source independently to measure the expansion history of the Universe. We show that by exploiting the clustering scale of the gravitational wave sources with galaxies of known redshift, we can infer the expansion history from redshift unknown gravitational wave sources. Using gravitational wave sources with unknown redshift that are detectable from the network of gravitational wave detectors with Advanced LIGO design sensitivity, we will be able to obtain accurate and precise measurements of the local Hubble constant, the expansion history of the universe, and the gravitational wave bias parameter, which captures the distribution of gravitational wave sources with respect to the redshift tracer distribution. This technique is not only limited to the low redshift gravitational wave sources, but will be also applicable to the high redshift gravitational wave sources detectable from Laser Interferometer Space Antenna (LISA), Cosmic Explorer (CE), and Einstein Telescope (ET). Moreover, this method is also going to be applicable to samples of supernovae and fast radio bursts with unknown or photometric redshifts.

I. INTRODUCTION

Measurement of the current expansion rate of the Universe, known as Hubble constant (denoted by H_0), as well as its value at different cosmological redshifts, is one of the key science goals in the field of Cosmology. This endeavour, which started with the first measurement of H_0 by Edwin Hubble [1], has been typically performed via electromagnetic probes which can be classified as standardized candles (e.g., supernovae (SNe)) [2–4], standard rulers (e.g., cosmic microwave background (CMB), baryon acoustic oscillation (BAO)) [5–9], and standard clock [10–13]. All these different probes have become increasingly successful in making precision measurements of H_0, but have failed to converge to a single value of the Hubble constant. In fact, low redshift probes to the Universe such as SNe [4] are indicating value of $H_0 = 74 \pm 1.4$ km/s/Mpc , whereas the probes which depend on the high redshift Universe such as big bang nucleosynthesis (BBN), CMB, BAO indicate value of Hubble constant $H_0 = 67.4 \pm 0.5$ km/s/Mpc [14, 15]. An independent measurement of $H_0 = 73.8^{+1.7}_{-1.8}$ km/s/Mpc from the time delay of the strongly lensed low redshift events by the H0LiCOW [16] also supports the mismatch. This discrepancy in the value of H_0 between the probes from the early-time Universe and probes from the late-time Universe differs by more than 4σ [17]. However independent measurements using the Tip of the Red Giant Branch (TRGB) as calibrators have indicated reduction in the discrepancy in the value of $H_0 = 69.8 \pm 0.8\,(\text{stat}) \pm 1.7\,(\text{sys})$ km/s/Mpc [18]. A few studies have also proposed the possible sources of systematic in the H_0 measurement from the late-time [19, 20]. However, there is as of yet no conclusive evidence that settles this mismatch by either any systematic, and/or invoking new physics, and hence independent probes are required to settle this discrepancy.

The direct detection of gravitational waves has recently provided a new independent probe of cosmic expansion. From the gravitational wave chirp generated by compact object binary mergers, one can infer luminosity distances [26, 27], leading to such sources being named standard sirens. The intrinsic luminosity of the gravitational wave source depends on the chirp mass, and its evolution with the frequency of the gravitational wave is solely dictated by the general theory of relativity [21, 22]. As a result, there is no need for additional calibration of the luminosity of the gravitational wave strain, apart from any systematic uncertainty arising from the gravitational wave detector calibration [28] and statistical uncertainty arising from the inclination angle [25].

Though standard sirens are promising, using them for the measurement of the expansion history requires an independent measurement of their redshift. The gravitational wave signal alone does not provide this information in the absence of a known scale arising from either tidal deformation [29] or mass-gap in the binary black

* s.mukherjee@uva.nl, mukherje@iap.fr
† bwandelt@iap.fr
‡ samaya.nissanke@uva.nl
§ silvestri@lorentz.leidenuniv.nl

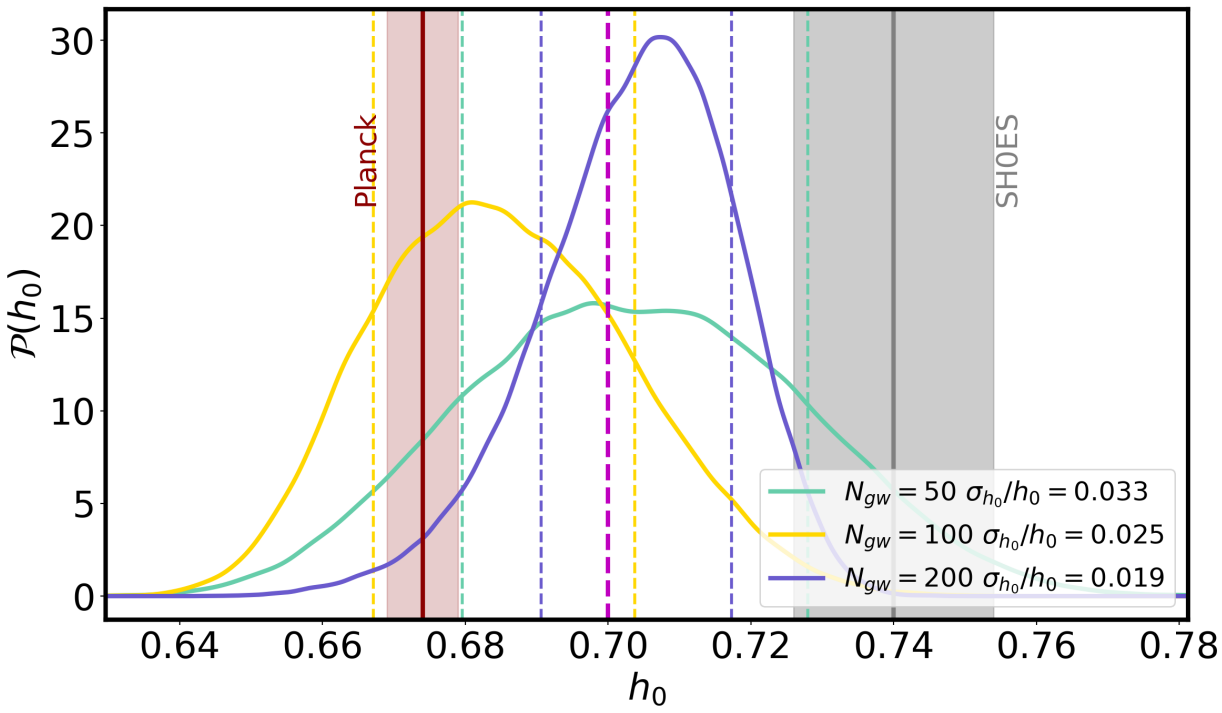

FIG. 1: We show the normalised posterior of the Hubble constant $H_0 = 100\,h_0$ km/s/Mpc for different number of gravitational wave sources distributed up to redshift $z = 0.5$ for the sky localization error $\Delta\Omega_{GW} = 10$ sq. deg after marginalizing over cosmological parameter Ω_m and nuisance parameters related to the gravitational wave bias parameters $b_{GW}(z)$. The constraints are also similar for $\Delta\Omega_{GW} = 25$ sq. deg. In vertical dashed line we show the region between 16^{th} and 84^{th} percentile of the distribution for each cases. The vertical magenta dashed line denotes the injected value of $h_0 = 0.7$ indicating reliable recovery in all cases. For comparison we also plot the measured value of $h_0 = 0.674 \pm 0.005$ by the Planck collaboration [8] and the value of $h_0 = 0.74 \pm 0.014$ by the SH0ES Team [4].

16-17
2 notes:

(BBH) sources due to pair instability supernova [30]. Another possibility to determine the redshift is by identifying the host galaxy using a coincident detection of

18

lectromagnetic (EM) counterpart from the gravitational wave source. This joint electromagnetic and gravitational wave measurement was done for the first time by the Laser Interferometer Gravitational-wave Observatory (LIGO) Scientific and Virgo Collaborations (LVC) from the binary neutron star merger GW170817 and led

uno SANCHEZ

n independent measurement of the Hubble constant

19

$= 70^{+12}_{-8}$ [14]. As shown in [31–33], the joint estimation of the electromagnetic signal and gravitational wave signal requires peculiar velocity correction to the gravitational wave sources. In general, the error bar on H_0

uno SANCHEZ

pre than 15% and, is currently not competitive with

20

measurements from CMB ($< 1\%$) and SNe ($\sim 1.5\%$). However in the future with the measurement of a large number of sirens (~ 50) with EM counterparts, one can achieve a 2% measurement of H_0 [34, 35]. Another avenue to reduce the error-bar on the value of H_0 is by the

uno SANCHEZ

surement of the inclination angle [1] by either measuring the two polarization states of the gravitational wave signal using an expanded network of three or more gravitational wave detectors [25] or by using the higher order multipole moments of the gravitational wave signal [36]. Measurement of the inclination angle is also possible by accurately modelling the EM emission from the jet of the gravitational wave source (e.g., [37–39], though note this method may introduce astrophysical modelling uncertainty.

Consistent with the single binary neutron star (BNS) detection with EM counterpart so far [40, 41], the expected number of gravitational wave sources with a EM counterpart in the cosmic volume that can be explored by the Advanced LIGO/Virgo and KAGRA detectors be small, since only BNS and neutron star black hole (NS-BH) systems are expected to have a detectable EM counterpart [42]. Also every BNS and NS-BH event may not

[1] The angle between the line of sight and the system's orbital angular momentum.

have a detectable EM counterpart e.g., [43–46][2]. Successful detection of the EM counterpart requires the flux of the EM counterpart to be higher than the detection threshold of follow-up telescopes, and also the sky localization area needs to be small enough to do a fast search of the EM counterpart before the EM counterpart fades away [47]. As a result, BNS and NS-BH systems which are farther away and have a poor sky localization may not have a detectable EM counterpart, similar to the BNS event [45]. These issues such as the rate of events, fainter EM counterparts, and poor sky localization can therefore be a serious bottleneck for measuring H_0 the expansion history of the Universe using gravitational waves sources on the time scale of ten years with an accuracy of $\sim 2\%$ [34, 35, 48].

Gravitational wave sources such as BBHs which have higher intrinsic luminosity than the BNS systems can be detected from farther away, granting us access to a larger detectable cosmic volume leading and, therefore, a higher possibility of detecting such systems. However, the majority of BBHs which are detectable in the frequency band of the Advanced LIGO/Virgo detectors are not expected to have EM counterparts from themselves, unless there is presence of baryons surrounding the BBH, where a candidate was recently announced [49]. We refer to the astrophysical systems without any EM counterparts as *dark standard sirens*. Due to the absence of the EM counterpart, identification of the host galaxy is not possible, and hence their redshift cannot be identified in the standard way. This implies that a large number of detected BBHs without EM counterparts cannot be used to measure the Hubble constant in the usual way by fitting the measured luminosity distance and redshift. An alternative approach is required to make these a useful probe of the expansion history of the Universe.

A possibility of using the dark standard sirens is to statistically obtain the host galaxy from galaxy catalogues [34, 50–52]. An application of this for the existing gravitational wave data was performed in previous studies [53–56]. These methods can be a promising way to obtain H_0 but are not optimal, as we will discuss in the following section. A forecast study of this method report the possibility of making H_0 measurement at the level of 1.2% in the future with 50 objects [34, 51, 55] [3] from only low redshift sources and keeping the value of matter density of the Universe Ω_m fixed. These methods associate a probability to each galaxy as a possible host of the dark sirens [55], and is only effective up to low redshift when the number of galaxies are limited. However, if the method is applied to the high redshift sources, then the possible host along a particular direction of the sky is going to be large, and as a result the method is not informative enough to choose the correct galaxy as a host. As a result, it restricts the use of dark sirens to low redshift even if accurate distance measurement is possible for sources at high redshift from the LIGO/Virgo design sensitivity [57, 58], and from the upcoming gravitational wave detectors such as Kamioka Gravitational Wave Detector (KAGRA) [59], LIGO-India [60], Laser Interferometer Space Antenna (LISA) [61], Einstein Telescope (ET) [62], and Cosmic Explorer (CE) [63]. An alternative way to find the redshift of the source is by exploring any mass scale associated with the compact objects originating due to neutron star mass distribution [64, 65], tidal deformation [29] or using the mass-gap in the gravitational wave source population due to the pair instability supernova [30].

In this work, we explore a method which can be applied up to high redshift (up to which galaxy samples are going to be available) and can measure the value of H_0 along with the density of dark energy, equation of state of dark energy, and also the spatial distribution of black holes with respect to the dark matter distribution. We exploit the fact that both the gravitational wave sources and galaxies are tracers of matter density, and therefore they are spatially correlated through the underlying matter field, to infer the redshift of the dark standard sirens [21, 66, 67]. We build on the previous work, where clustering with galaxies was applied to redshift unknown (or photometrically known) SNe [67]. Our method does not identify *the host galaxy* of the BBH source, but finds *the host redshift shell* by exploring the three-dimensional spatial cross-correlation of the gravitational wave sources with redshift-known galaxies. Host galaxy identification is therefore in the limit of our approach that only exploits the small, galaxy-scale correlations [21].

We detail the formalism of this method and the likelihood setup in Sec. II and Sec. III respectively. Our method does not require making any additional assumption about the redshift dependence of the merger rate of gravitational waves sources but only requires that the BBH mergers traces galaxies (incorporating the possibility of natal birth kicks), so that there is a spatial correlation, as discussed in Sec. IV. We show a forecast for the accuracy and precision of the measurements of H_0 achievable with our method in Fig. 1 after marginalizing over the matter density Ω_m, and the redshift dependent gravitational wave bias parameter $b_{GW}(z) = b_{GW}(1+z)^{\alpha}$. Details about this result are given in Sec. V. Moreover, since dark sirens can be detected up to high redshift, this method makes it possible to also explore the expansion history of the Universe and can provide an independent measurement of the cosmological parameters related to matter density Ω_m, dark energy equation of state w_0, and its redshift dependence $w(z) = w_a(z/(1+z))$. This method can also explore the bias parameter of the gravitational wave sources at different redshifts $b_{GW}(z)$, which will capture its spatial distribution with respect to dark

[2] The nature of the lighter companion of the binary system for GW190814 [46] is most likely a black hole. However, at present, the data and models for neutron star equation-of-states cannot conclusively exclude the possibility it is a neutron star.

[3] Scaling the previous bounds from [34] and [55] as $1/\sqrt{N_{GW}}$ indicates similar error-bar.

matter. This method will also be applicable to the multi-messenger test of gravity proposed previously [68, 69]. The breadth of the scientific returns possibly from this avenue surpasses the statistical host identification methods [34, 51, 55]. For comparison, we apply our method to only low redshift sources with fixed value of Ω_m, assuming a known value of the gravitational wave bias parameter b_{GW}. We find that the the error-bar on H_0 from these methods [34, 51, 55] is more by only about 30% than our method. This implies in the limit of low redshift sources, these methods [34, 51, 55] approach the optimal solution proposed in this work. We conclude in Sec. VI.

39

uno SANCHEZ

II. FORMALISM: EXPLORING THE CLUSTERING OF THE GRAVITATIONAL WAVE SOURCES WITH GALAXIES

The matter distribution is clustered and can be statistically described by the correlation function $\xi(r)$[4] [70–74]. Astrophysical gravitational wave events are expected to occur in galaxies, and hence are going to follow the spatial distribution of the galaxies with a bias parameter b_{GW} [5] is different from the bias parameters for galaxies b_g. According to the standard model of cosmology, the spatial distribution of galaxies should trace the underlying distribution of matter in the Universe, and can be expressed as a biased tracer of the matter density field $\delta_m(\boldsymbol{k})$ by the relation,

40-41
2 notes:

42-43
2 notes:

$$\delta_g(\boldsymbol{k}) = b_g(k)\delta_m(\boldsymbol{k}), \tag{1}$$

where $b_g(k)$ is the galaxy bias, $\delta_g(\boldsymbol{k})$ is the Fourier transformation of the real space galaxy density field defined in terms of the number density of galaxy $n_g(\hat{r})$ at a position $\boldsymbol{r}$ and mean number of galaxies $\bar{n}_g$.[6] as $\delta_g(\boldsymbol{r}) = n_g(\boldsymbol{r})/\bar{n}_g - 1$ A spectroscopic (or photometric) survey results in observations of galaxies in the redshift space denoted by superscript s, which leads to a redshift space distortion (RSD) in the density field [75]. The large scale effect due to RSD (known as the Kaiser term) [75, 76] is

$$\delta_g^s(\boldsymbol{k}, z) = b_g(k, z)(1 + \beta_g \mu_{\hat{k}}^2)\delta(\boldsymbol{k}, z), \tag{2}$$

where $\beta \equiv f/b_g(k, z)$ defined in terms of $f \equiv \frac{d\ln D}{d\ln a}$ which is the logarithmic derivative of the growth function D with respect to the scale factor a, $\mu_{\hat{k}} = \cos\hat{n}.\hat{k}$ is angle between the line of sight and the Fourier mode $\hat{k}$, and the superscript r denotes real space. Following the definition Eq. (1), we can define the density field for the gravitational wave sources in real space δ^r_{GW} as

$$\delta^r_{GW}(\boldsymbol{k}, z) = b_{GW}(k, z)\delta(\boldsymbol{k}, z) \tag{3}$$

where $b_{GW}(k, z)$ is the gravitational wave bias parameter [32, 67, 77–79]. The gravitational wave bias parameter captures how gravitational wave sources trace the large scale structure in the Universe [77]. Since the gravitational wave sources are tracers of luminosity distance and not redshift, they are not affected by RSD. The corresponding power spectrum between the field can then be written as

44

uno SANCHEZ

$$\left\langle \begin{pmatrix} \delta_g^s(\boldsymbol{k}, z) \\ \delta^r_{GW}(\boldsymbol{k}, z) \end{pmatrix} \begin{pmatrix} \delta_g^s(\boldsymbol{k}', z) & \delta^r_{GW}(\boldsymbol{k}', z) \end{pmatrix} \right\rangle = \begin{pmatrix} P^{ss}_{gg}(\boldsymbol{k}, z)\delta_D(\boldsymbol{k} - \boldsymbol{k}') + \bar{n}_g(z)^{-1} & P^{sr}_{g\,GW}(\boldsymbol{k}, z)\delta_D(\boldsymbol{k} - \boldsymbol{k}') \\ P^{sr}_{g\,GW}(\boldsymbol{k}, z)\delta_D(\boldsymbol{k} - \boldsymbol{k}') & P^{rr}_{GW\,GW}(\boldsymbol{k}, z))\delta_D(\boldsymbol{k} - \boldsymbol{k}') + \bar{n}_{GW}(z)^{-1} \end{pmatrix}, \tag{4}$$

where $P^{ij}_{xy}(\boldsymbol{k}, z)$ is the three dimensional power spectrum at redshift z associated with the clustering between two tracers ($\{x\,y\} \in \{g, GW\}$) in redshift space or real space ($\{i\,j\} \in \{s, r\}$), $\delta_D(\boldsymbol{k} - \boldsymbol{k}')$ denotes the Dirac delta function, and $\bar{n}_x(z)^{-1}$ is the shot noise contribution which is non-zero only when x and y are the same. The redshift tomographic estimate of the auto power spectrum ($x = y$) and cross power spectrum ($x \neq y$) between galaxies and gravitational wave sources can be written in terms of the matter power spectrum $P_m(k, z)$ as

45-46
2 notes:

$$\begin{aligned} P^{ss}_{gg}(\boldsymbol{k}, z) &= b_g^2(k, z)(1 + \beta_g\mu_{\hat{k}}^2)^2 P_m(k, z), \\ P^{sr}_{g\,GW}(\boldsymbol{k}, z) &= b_g(k, z)b_{GW}(k, z)(1 + \beta_g\mu_{\hat{k}}^2)P_m(k, z), \\ P^{rr}_{GW\,GW}(\boldsymbol{k}, z) &= b_{GW}^2(k, z)P_m(k, z). \end{aligned} \tag{5}$$

Due to the presence of redshift space distortion (RSD) the observed auto (and cross) power spectrum with galaxies are anisotropic. The bias parameter for galaxies $b_g(k, z)$ and gravitational wave sources $b_{GW}(k, z)$ are modelled as redshift and scale-dependent. At large scales ($k < 0.1$) the galaxy bias is scale-independent, and behaves like a constant value $b_g = 1.6$ [80–82]. For the sources of gravitational wave, we can also expect similar

47-48
2 notes:

[4] Correlation function $\xi(r)$ is related to the power spectrum $P(k)$ by Fourier Transformation.

[5] If primordial black holes (PBHs) are dark matter, then the distribution of PBHs are also going to be biased tracer of the galaxy distribution.

[6] $\bar{n}_g \equiv N_g/V_s = \sum_i n_g(\boldsymbol{r}_i)$

scale-independent behaviour of the bias parameter b_{GW} in the large scales. However, at the small scales, the bias parameter is likely to be scale-dependent. The redshift dependence of the gravitational wave bias parameter is also unknown and we will discuss its implication in detail in the next section.

One of the key aspects of Eq. (5) is that the underlying cross power spectrum between galaxies and gravitational wave sources $P^{sr}_{g\,GW}(\boldsymbol{k}, z)$ is related to the matter power spectrum $P_m(k, z)$, which is also measurable from the auto power spectrum of galaxies $P^{ss}_{gg}(\boldsymbol{k}, z)$. As a result, $P_{g\,GW}(\boldsymbol{k}, z)$ should follow similar statistical properties as $P^{ss}_{gg}(\boldsymbol{k}, z)$. We exploit this very simple model to use the spatial cross-correlation of galaxies with gravitational wave sources to infer the luminosity-distance–redshift relation and hence the cosmological parameters.

III. LIKELIHOOD FOR INFERRING THE EXPANSION HISTORY USING DARK STANDARD SIRENS

Let us consider a sample of N_{GW} gravitational wave sources (denoted by i) for which we have inferred the luminosity distance $\{d_l\}$ to the source over a sky volume denoted by V_s. For each of these sources there is also a measurement of the localization error with a 68% sky localization error $\Delta\Omega$ for each source. The presence of sky localization error will smooth out the density fluctuations for values of $k > k_{eff}(z) \equiv \sqrt{8\ln 2}/(\Delta\Omega_{GW}\, d_c(z))$, where $d_c(z)$ is the comoving distance to the source.[7] Critically, assuming a Gaussian distribution of the sky localization error, we can write the effect of sky localization on the density field as $\delta_{GW}(\boldsymbol{k}, \Delta\Omega_{GW}, z) = \delta_{GW}(\boldsymbol{k}, z)e^{-k^2/k_{eff}^2(z)}$. Along with the gravitational wave sources, we consider number of galaxy samples $N_g = \bar{n}_g V_s$ in the overlapping sky volume V_s with the known redshift z_g and an error σ_z and the sky position denoted by $\{\theta_g, \phi_g\}$ with an error on the sky position $\Delta\Omega_g$.[8] Using galaxies samples with known redshift we can make tomographic bins of the galaxies with N_g galaxies in each redshift bin.

The expansion history of the Universe ($H(z) = H_0(\Omega_m(1+z)^3 + \Omega_{de}\exp(3\int_0^z d\ln(1+z)(1+w(z))))^{0.5}$ and the corresponding cosmological parameters ($\Theta_c \in \{H_0,\, \Omega_m,\, w(z) = w_0 + w_a(z/(1+z))\}$) can be explored from dark standard sirens using the Bayes theorem [83]

$$\mathcal{P}(\Theta_c|\boldsymbol{\vartheta}_{GW}, \boldsymbol{d}_g) \propto \iint d\Theta_n\, dz \left[\prod_{i=1}^{N_{GW}} \mathcal{L}(\boldsymbol{\vartheta}_{GW}|P^{ss}_{gg}(\boldsymbol{k}, z), \Theta_n, \boldsymbol{d}_g(z))\mathcal{P}(\boldsymbol{d}_g|P^{ss}_{gg}(\boldsymbol{k}, z))\mathcal{P}(\{d_l^i\}_{GW}|z, \Theta_c, \{\theta^i,\, \phi^i\}_{GW})\Pi(z)\right] \times \Pi(\Theta_n)\Pi(\Theta_c), \tag{6}$$

where, the gravitational wave data vector is composed of $\boldsymbol{\vartheta}_{GW} \equiv \{d_l^i,\, \theta^i_{GW},\, \phi^i_{GW}\}$ and the galaxy data vector is composed of $\boldsymbol{d}_g \equiv \{\delta_g(z^i_g,\, \theta^i_g,\, \phi^i_g)\}$. $\Pi(\Theta_c)$ and $\Pi(\Theta_n)$ denotes respectively the prior on the cosmological parameters Θ_c and prior on the nuisance parameters $\Theta_n \equiv \{b_{GW}(k, z)\}$. $\Pi(z)$ denotes the prior on the redshift range of the gravitational wave sources which can be taken uniform over a wide range. In the presence of a redshift information about the gravitational wave sources, an informative prior on the redshift can be considered. In this analysis we consider a uniform prior $\mathcal{U}(0, 1)$[9] on the redshift unknown gravitational wave sources; this is sufficiently wide for the near-term and medium-term gravitational wave surveys we are considering.

$\mathcal{P}(\{d_l^i\}_{GW}|z, \Theta_c)$ is the posterior on the luminosity distance d_l from the gravitational wave data $\boldsymbol{\vartheta}_{GW}$ which, for convenience, we model as a Gaussian distribution.[10]

$$\mathcal{P}(\{d_l^i\}_{GW}|z,\Theta_c, \{\theta^i,\, \phi^i\}_{GW}) \propto \exp\left(-\frac{(d_l^i(\{\theta^i,\, \phi^i\}_{GW}) - d_l(z, \Theta_c))^2}{2\sigma^2_{d_l}}\right), \tag{7}$$

where, σ_{d_l} is the error on the luminosity distance, and $d_l(z, \Theta_c) = (1+z)\int_0^z \frac{c\,dz'}{H(z')}$ is the model for the luminosity distance. The posterior of the galaxy density field $\mathcal{P}(\boldsymbol{d}_g|P_{gg}(\boldsymbol{k}, z))$ given the galaxy power spectrum $P_{gg}(\boldsymbol{k}, z)$ (mentioned in Eq. (6)) can be written as

$$\mathcal{P}(\boldsymbol{d}_g|P^{ss}_{gg}(\boldsymbol{k}, z)) \propto \exp\left(-\frac{\delta^s_g(\boldsymbol{k}, z)\delta^{s*}_g(\boldsymbol{k}, z)}{2(P^{ss}_{gg}(\boldsymbol{k}, z) + n_g(z)^{-1})}\right), \tag{8}$$

[7] Comoving distance $d_c(z)$ is related to the luminosity distance $d_l(z)$ by the relation $d_l(z) = (1+z)d_c(z)$.

[8] For all practical purpose, sky localization error for galaxies can be considered to be zero.

[9] $\mathcal{U}(a, b)$ denotes the uniform function over the range (a,b).

[10] While this posterior is likely to be non-Gaussian in practice, we make this assumption purely to construct a forecast that can be compared to other studies making similar assumptions.

where $\delta_g^s(\boldsymbol{k},z) = \int d^3\boldsymbol{r}\,\delta_g(\boldsymbol{r})e^{i\boldsymbol{k}.\boldsymbol{r}}$ is the Fourier decomposition of the galaxy distribution, the first term in the denominator $P_{gg}^{ss}(\boldsymbol{k},z)$ is the galaxy three dimensional power spectrum defined in Eq. (4), and $n_g(z) = N_g(z)/V_s$ is the number density of galaxies in the redshift bin z. The likelihood term $\mathcal{L}(\boldsymbol{\vartheta}_{GW}|P_{gg}(\boldsymbol{k},z),\Theta_n,\boldsymbol{d}_g(z))$ in Eq. (6) is

$$\mathcal{L}(\boldsymbol{\vartheta}_{GW}|P_{gg}^{ss}(\boldsymbol{k},z),\Theta_n,\boldsymbol{d}_g(z)) \propto \exp\Bigg(-\frac{V_s}{4\pi^2}\int k^2dk\int d\mu_k \frac{\Big(\hat{P}(\boldsymbol{k},\Delta\Omega_{GW}) - b_g(k,z)b_{GW}(k,z)(1+\beta_g\mu_{\hat{k}}^2)P_m(k,z)e^{-\frac{k^2}{k_{eff}^2}}\Big)^2}{2(P_{gg}^{ss}(\boldsymbol{k},z)+n_g(z)^{-1})(P_{GW\,GW}^{rr}(\boldsymbol{k},z)+n_{GW}(z)^{-1})}\Bigg), \tag{9}$$

where $\hat{P}(\boldsymbol{k},z) = \delta_g(\boldsymbol{k},z)\delta_{GW}^*(\boldsymbol{k},\Delta\Omega_{GW})$, $n_{GW}(z) = N_{GW}(d_l^i(z))/V_s$ is the number density of gravitational wave sources denoted in terms of the number of number of objects in the luminosity distance bin $N_{GW}(d_l^i(z))$, and V_s denotes the total sky volume. The likelihood given in Eq. (9) is maximized for that set of cosmological parameters that transforms the galaxy density field from redshift space to match or correlated maximally with the spatial distribution of gravitational wave sources.

The integration in Eq. (9) takes into account the anisotropic shape of the power spectrum by combining the contribution from $\mu_k = \cos\hat{n}.\hat{k}$ arising due to RSD. The total number of Fourier modes which contributes to the signal depends on the volume of the sky survey given by $N_m = k^2dkV_s/4\pi^2$. In the limit $n_x(z)P_x(k,z) > 1$, the likelihood is in the cosmic variance limited regime, and in the other extreme scenario $n_x(z)P_x(k,z) < 1$, it is in the shot noise dominated regime. For the gravitational wave sources expected within 5 years (with an event rate $R(z) = 100$ Gpc^{-3} yr^{-1} [84, 85]), we are going to explore the cross-correlation between the galaxies and gravitational wave sources only for small values of $k < k_{eff}$ in the shot noise regime $n_{GW}P_{GW\,GW}^{ss}(k,z) < 1$. Galaxy samples are going to be have $\mathcal{O}(10^9)$ galaxies [86–92] and as a result, we are going to be in the cosmic variance limited regime for the values of $k < k_{eff}$. So, the denominator of the exponent in Eq. (9), is going to scale as $\frac{4\pi^2P_{gg}^{ss}(\boldsymbol{k},z)}{n_{GW}(z)}$. With the availability of the large number of gravitational wave samples, the measurement is going to be in the cosmic variance limited regime $n_{GW}P_{GW\,GW}^{rr}(k,z) > 1$, and in that case the denominator of the exponent can be approximated as $4\pi^2P_{gg}^{ss}(\boldsymbol{k},z)P_{GW\,GW}^{rr}(\boldsymbol{k},z)$. In this analysis, we have considered an analytical covariance matrix. This can be also calculated from simulations for a specific mission of large scale structure and gravitational waves experiment.

IV. GENERATION OF MOCK SAMPLE

We implement our method on a mock sample of large scale structure and gravitational wave sources which are produced for the log-normal distribution of the density field using the publicly available package `nbodykit` [93]. The realization of the galaxies and gravitational wave sources are obtained from the same random realization, using a fixed matter power spectrum $P_m(\boldsymbol{k},z)$ with different bias parameters for galaxies and gravitational wave sources b_g and b_{GW} respectively. In this analysis, we use the mock samples with the box length (in units of Mpc/h) $[l_x = 1350., l_y = 1350., l_z = 300]$ from redshift range $z = 0$ to $z = 1.0$ with Planck-2015 cosmology [8]. These mocks do not take into account the contribution from weak lensing. Weak lensing is going to have a marginal ($\leq 1\%$) increase in the variance of the inferred cosmological parameters for the low redshift gravitational wave sources considered in this analysis.

Galaxy samples: The galaxy samples are produced for a scale-independent bias parameter $b_g = 1.6$ including the effect from RSD [93]. The galaxy mocks are obtained for the number of galaxies $N_g = 1.5\times10^4$. The redshift of these sources is assumed to be known spectroscopically, which implies the corresponding error in the redshift measurement is $\sigma_z \approx 0$.

Gravitational wave samples: For the same set of cosmological parameters and using the same realization of the large scale structure density field for which galaxy samples are produces, we obtain the gravitational wave samples N_{GW} [11] with the gravitational wave bias parameter $b_z = b_{GW}(1+z)^\alpha$ with $b_{GW} = 2$ and $\alpha = 0$. For these samples we consider three different cases of sky localization error $\Delta\Omega_{GW} = 10$ sq. deg., $\Delta\Omega_{GW} = 25$ sq. deg., and $\Delta\Omega_{GW} = 100$ sq. deg. [94, 95] which are possible to achieve from the network of five gravitational wave detectors (LIGO-Hanford, LIGO-Livingston, Virgo, KAGRA, LIGO-India [57–60]). For each gravitational wave

[11] Different cases of N_{GW} are considered in this analysis, and are discussed in the respective sections

sources, the fractional error on the luminosity distance depends inversely on the matched filtering signal-to-noise ratio (ρ) [25, 96–99]

$$\rho^2 \equiv 4 \int_0^{f_{max}} df \frac{|h(f)|^2}{S_n(f)}, \tag{10}$$

where the value of f_{max} is considered as $f_{merg} = c^3(a_1\eta^2 + a_2\eta + a_3)/\pi GM$ [100] [12], $S_n(f)$ is the detector noise power spectrum, which we consider as the advance LIGO design sensitivity [58] [13]. The template of the gravitational wave strain $h(f)$ for $f \leq f_{merg}$ can be written in terms of the redshifted chirp mass $\mathcal{M}_z = (1+z)\mathcal{M}_c$, inclination angle with respect to the orbital angular momentum $\hat{L}.\hat{n}$ (which is denoted by the function $\mathcal{I}_\pm(\hat{L}.\hat{n})$), and luminosity distance to the source d_L by the relation [97, 100–103]

$$h_\pm(f) = \sqrt{\frac{5}{96}} \frac{G^{5/6}\mathcal{M}_z^2 (f_z \mathcal{M}_z)^{-7/6}}{c^{3/2}\pi^{2/3} d_L} \mathcal{I}_\pm(\hat{L}.\hat{n}). \tag{11}$$

In this analysis, we critically consider the posterior distribution of luminosity distance to be Gaussian with the minimum matched filtering detection threshold $\rho_{th} = 10$ for equal mass binaries with masses $30\,M_\odot$.[14] The fractional error in the luminosity distance σ_{d_l}/d_l can be about 10% for the bright sources having high detection SNR $\rho > 60$ and be large as 70% for the objects at detection threshold $\rho = 10$. The mean value of the luminosity distance are kept for the flat LCDM cosmological model with the parameter values [$H_0 = 70\,\mathrm{km/s/Mpc}$, $\Omega_m = 0.315$, $\Omega_\Lambda = 1 - \Omega_m, w_0 = -1, w_a = 0$]. The values of the Hubble parameter is kept completely different from the value of H_0 considered in the large scale structure mock sample ($H_0 = 67.3$ km/s/Mpc) to show that the inferred cosmological parameters are affected only by the luminosity distance and not by the parameters assumed in the mock catalog. For the gravitational wave sources, we do not assume any redshift information. The current estimate of the event rate of BBHs is $R(z) = 10^2$ Gpc^{-3} yr^{-1} [84]. With this event rate, we expect to see a few thousands events detected per year with the advanced LIGO design sensitivity [58]. In this analysis, we show the measurability of the expansion history considering a few different cases of the number of gravitational wave sources N_{GW}[15] and for the sky localization which is expected to be achievable with a network of four/five gravitational detectors.

[12] $M = m_1 + m_2$ is the total mass of the coalescing binaries, η is the symmetric mass ratio $\eta = m_1 m_2/M^2$, c is the speed of light and G denotes the gravitational constant. The value of the parameters are $a_1 = 0.29740$, $a_2 = 0.044810$, $a_3 = 0.095560$ [100].

[13] The noise curves are available publicly in this website https://dcc-lho.ligo.org/LIGO-T2000012/public

[14] $M_\odot = 2 \times 10^{30}$ kg denotes the mass of the sun.

[15] We consider four cases of $N_{GW} = 50, 100, 200, 280$ for this analysis in the LIGO design sensitivity, which is expected to be easily available with the network of gravitational wave detectors.

V. RESULTS

Using the mock samples of galaxies and gravitational wave sources, discussed in Sec. IV, we explore the cosmological parameters which affects the expansion history of the Universe[16] (Hubble constant H_0, matter density Ω_m, dark energy equation of state $w(z)$) using the formalism described in Sec. III. The precise and accurate inference of the cosmological parameters using this method will rely on successfully mitigating the uncertainties associated with the unknown bias parameter and its redshift dependence associated with the gravitational wave sources. So, along with the cosmological parameters, we also consider the gravitational wave bias parameter to be unknown $b_{GW}(z) = b_{GW}(1+z)^\alpha$ and jointly infer the value of b_{GW} and α (these are our nuisance parameters $\Theta_n \in \{b_{GW}, \alpha\}$) in the analysis along with the cosmological parameters. We consider three cases in this analysis: (i). H_0, Ω_m, with fixed $w_0 = -1$, and $w_a = 0$; (ii). Ω_m and Ω_Λ, with fixed $H_0 = 70$ km/s/Mpc, $w_0 = -1$, and $w_a = 0$; (iii). w_0 and w_a with fixed $H_0 = 70$ km/s/Mpc and $\Omega_m = 0.315$. Uniform priors on the cosmological and nuisance parameters are considered in the following range: $\Pi\left(\frac{H_0}{\mathrm{km/s/Mpc}}\right) = \mathcal{U}(20, 150)$, $\Pi(\Omega_m) = \mathcal{U}(0.1, 1)$, $\Pi(\Omega_\Lambda) = \mathcal{U}(0, 1)$, $\Pi(w_0) = \mathcal{U}(-2, 0)$, $\Pi(w_a) = \mathcal{U}(-8, 8)$, $\Pi(b_{GW}) = \mathcal{U}(0, 6)$, $\Pi(\alpha) = \mathcal{U}(-4, 4)$ and $\Pi(z) = \mathcal{U}(0, 1)$. We show the results only for the $\Delta\Omega_{GW} = 10$ sq. deg. However, the results for $\Delta\Omega_{GW} = 25$ sq. deg. only deteriorates marginally. For sky-localization error $\Delta\Omega_{GW} = 100$ sq. deg., the impact on the error-bars for the bias parameters are about a factor of two, and is less for other parameters.

A. Measurement of H_0, Ω_m and $b_{GW}(z)$

The joint-estimation of the cosmological parameters H_0 and Ω_m along with the nuisance parameters are shown in Fig. 2 for fixed value of $w_0 = -1$ and $w_a = 0$. These results are obtained for the cases with $N_g = 1.5 \times 10^4$, $N_{GW} = 200$ [17], and $\Delta\Omega_{GW} = 10$ sq. deg [18]. The results show that we can make the measurement of $H_0 = 70$ km/s/Mpc with an accuracy of 1.9% with only $N_{GW}(z) = 40$ BBHs in each redshift bin of width $\Delta z = 0.1$ up to redshift $z = 0.5$ detectable with the advance LIGO design sensitivity [58]. The result shown in Fig. 2 also indicates that the gravitational wave bias parameters b_{GW} and α are uncorrelated with the cosmological parameters H_0 and Ω_m. As a result, uncertainty associated with the gravitational wave bias parameter

[16] Considering only the cosmological models with curvature $\Omega_K = 0$.

[17] The total number of gravitational wave sources $N_{GW} = \int N(z)dz$.

[18] Results with $\Delta\Omega_{GW} = 25$ sq. deg changes only marginally.

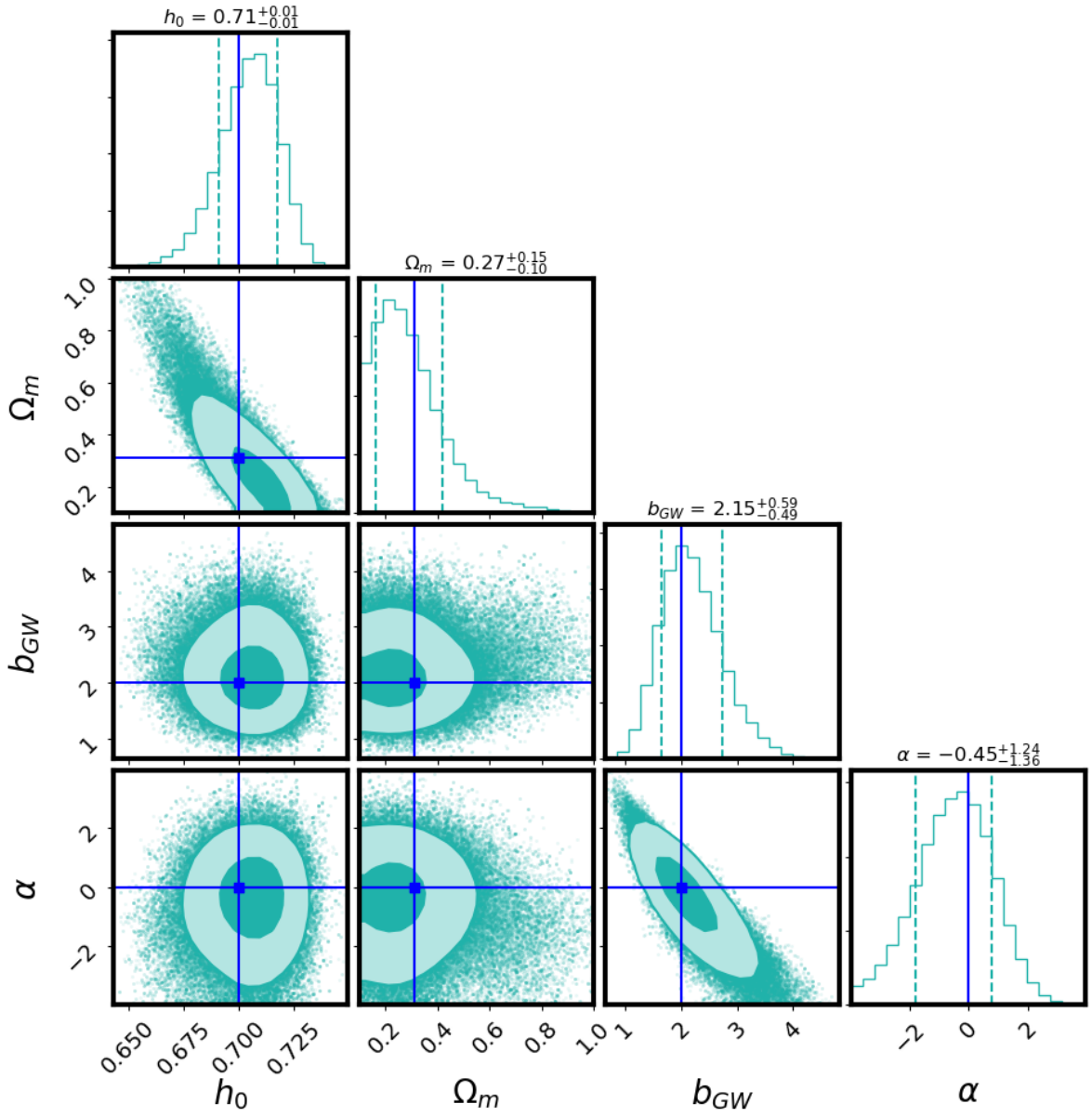

FIG. 2: We show the joint posterior of the cosmological parameters $H_0 = 100h_0$ km/s/Mpc and Ω_m along with the nuisance parameters related to the gravitational wave bias parameter $b_{GW}(z) = b_{GW}(1+z)^{\alpha}$ for number of gravitational wave sources $N_{GW}(z) = 40$ extended up to redshift $z = 0.5$, and sky localization error $\Delta\Omega_{GW} = 10$ sq deg. The 68%, and 95% contours are shown in these plots along with the input values by the blue line. The mean value along with 1σ error-bar are mentioned in the title of the posterior distribution for all the parameters. Other cosmological parameters such as $w_0 = -1$ and $w_a - 0$ are kept fixed for these results.

79-80
2 notes:

81-82
2 notes:

83

uno SANCHEZ

does not affect the inference of the cosmological parame- (for the parametric form of the bias considered in this analysis). This makes our method both precise and accurate to infer the cosmological parameters. Using this method we can measure the value of the gravitational wave bias parameter with an $\sigma_{b_{GW}}$ $\sim$ 27% with only 200 BBHs at the advanced LIGO design sensitivity [58]. The cross-correlation technique makes it possible to measure the bias parameter even with the currently ongoing detector network and much before the operation of next-generation gravitational wave detectors [62, 63] by using the auto correlation between the gravitational wave sources. This is an another additional gain which is not possible from the other proposed methods [34, 51, 55].

The forecast posteriors on H_0 (after marginalizing over Ω_m, b_{GW}, α) for $N_{GW} = 50, 100, 200$ gravitational wave sources are shown in Fig. 1 along with the measured of Hubble constant $H_0 = 67.4 \pm 0.5$ km/s/Mpc and

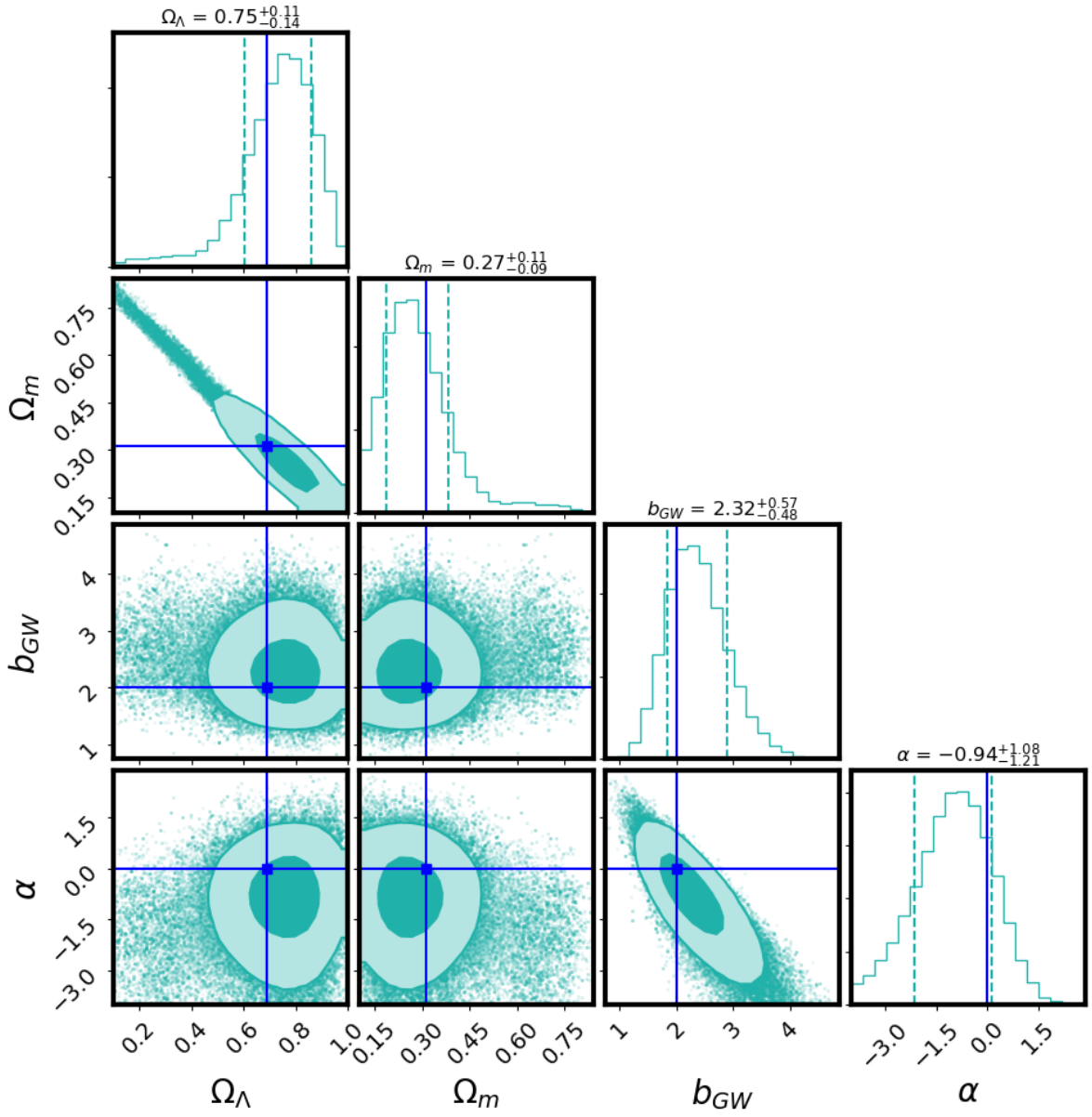

FIG. 3: We show the joint posterior of the cosmological parameters Ω_Λ and Ω_m along with the nuisance parameters related to the gravitational wave bias parameter $b_{GW}(z) = b_{GW}(1+z)^\alpha$ for number of gravitational wave sources $N_{GW}(z) = 40$ extended up to redshift $z = 0.7$, and sky localization error $\Delta\Omega_{GW} = 10$ sq deg. The 68%, and 95% contours are shown in these plots along with the input values by the blue line. The mean value along with 1σ error-bar are mentioned in the title of the posterior distribution for all the parameters. Other cosmological parameters such as $H_0 = 70$ km/s/Mpc, $w_0 = -1$ and $w_a = 0$ are kept fixed for these results.

84

uno SANCHEZ

$H_0 = 74 \pm 1.4$ km/s/Mpc from Planck [15] and SH0ES [4] respectively. The uncertainty in the measurement of H_0 decreases as the number of sources increases ($\sim N_{GW}^{-1/2}$) and as the uncertainty in the luminosity distances decreases ($\sim \sigma_{d_l}/d_l$).

85-86

2 notes:

Fig.1 shows that a measurement of H_0 from 200 dark sirens ($\sigma_{H_0}/H_0 = 1.9\%$) compares favourably with that which would be obtained from 50 sources *with EM counterparts* (such as BNS and NS-BH, assuming $\sigma_{H_0}/H_0 =$ 2%, [34, 35]). However, as the number of detected dark sirens is expected to outnumber the sources with EM counterparts (such as BNSs and NS-BHs), one can expect the constraints on H_0 from dark sirens to dominate those from BNSs and NS-BHs, with very conservative assumptions about the availability of galaxy redshift survey covering a substantial fraction of the sky. *In summary, the H_0 our method is going to provide both accurate and precise measurements of H_0 from dark sirens*

along with Ω_m, and redshift dependent gravitational wave bias parameter $b_{GW}(z)$ from the network of the advanced with/without optical squeezing gravitational wave detectors. Combining these two independent constraints would achieve $\sigma_{H_0} \sim 1.4\%$, which is competitive with current constraints from standard candles [4].

87-89
3 notes:

B. Measurement of Ω_Λ, Ω_m and $b_{GW}(z)$

As our method can be applied to high redshift (up to which galaxy surveys will be available), we can also measure the energy budget in dark energy Ω_Λ from dark sirens. We make the joint estimation of the cosmological parameters Ω_Λ–Ω_m along with the two bias parameters b_{GW} and α for the parametric form $b_{GW}(z) = b_{GW}(1+$ for a fixed value of $H_0 = 70\,\mathrm{km/s/Mpc}, w_0 = -1$ and $= 0$ with $N_{GW}(z) = 40$ up to redshift $z = 0.7$. The corresponding plot is shown in Fig. 3. We show for the first time that the energy budget of dark energy can be measured from using dark sirens detectable within the earliest timescale with the advanced LIGO design sensitivity [58] with only $N_{GW} = 280$ BBHs. The Ω_m and Ω_Λ are also uncorrelated with the bias parameters (b_{GW} and α), and as a result will not affect the measurement of cosmological parameters. The measurement of Ω_Λ and Ω_m gets less constraining for the limited number of gravitational wave sources if the value of H_0 is not kept fixed. However, joint estimation with H_0 is possible with more gravitational wave sources. This method is also useful for the future gravitational wave detectors such as LISA [61], ET [62], and CE [63] to measure Ω_Λ, Ω_m, and the gravitational wave bias parameter $b_{GW}(z)$.

90
uno SANCHEZ
91
uno SANCHEZ
92-93
2 notes:

C. Measurement of w_0, w_a and $b_{GW}(z)$

The two-parameter phenomenological model of the dark energy equation of state $w_{de} = w_0 + w_a\, z/(1+z)$ is usually considered to explore the redshift dependence of dark energy. Using our method, we show the joint estimation of w_0 and w_a along with the two bias parameters b_{GW} and α (for the parametric form $b_{GW}(z) =$ $(1+z)^\alpha$) in Fig. 4 for $N_{GW}(z) = 40$ extended up to 0.7. We have kept the value of $H_0 = 70$ km/s/Mpc and $\Omega_m = 0.315$ fixed for flat LCDM model. This plot shows that this technique is capable to infer the dark energy equation of state with $N_g = 1.5 \times 10^4$, $N_{GW} = 280$ (up to redshift $z = 0.7$) for $\Delta\Omega_{GW} = 10$ sq. deg. The constraints on the values on $w_0 = -1$ are possible with , however the constraints on w_a are going to be weak the modest number of gravitational wave sources. With more number of gravitational wave sources possible from the five years of observation with the Advanced LIGO design sensitivity [58], we will be able to infer the dark energy equation of state with higher accuracy (the error on the parameter reduces by $N_{GW}^{-1/2}$) for sources up to redshift $z \sim 1$. This independent avenue to measure w_0 and w_a will also beaccessible from the next generation gravitational wave detectors such as LISA [61], ET [62], and CE [63] for sources which are beyond redshift $z = 1$. The gravitational wave bias parameters b_{GW} and α are also uncorrelated with the parameters describing dark energy equation of state and can be measured high statistical significance as shown in Fig. 4.

94
uno SANCHEZ
95
uno SANCHEZ
96
uno SANCHEZ

VI. CONCLUSIONS AND DISCUSSIONS

Gravitational-wave sources are accurate luminosity distance tracers without requiring any external calibration, if instrument calibration can be achieved [28]. This makes gravitational wave sources an exquisite probe to measure the expansion history of the Universe by exploiting the luminosity distance and its redshift. However, inference of the redshift of the gravitational wave sources requires either an EM counterpart or a known mass scale (such as the mass scale associated with the tidal deformation [29] and mass scale associated with the pair instability of supernova [30]) to infer the redshift. However, for most of the gravitational wave sources, measurement of the mass scale is not going to be possible. The alternative method to infer the redshift of the gravitational wave sources by exploiting the scale associated with the three dimensional clustering property of cosmic structures [67]. In this paper, we show the applicability of this avenue for the gravitational wave sources to infer the expansion history of the Universe.

Using the detector sensitivity expected from the current generation gravitational wave detectors [57–60], we show that with the modest number of gravitational wave sources (~ 100) we will be able to infer the Hubble constant H_0 with an accuracy $\sim 2.5\%$ as shown in Fig. 1 for gravitational wave sources distributed up to redshift $z = 0.5$. The exploration of the clustering of the gravitational wave sources with the galaxies makes it a robust method to infer the Hubble constant using the dark sirens. Going beyond Hubble constant, our method makes it possible to measure the fraction of dark energy in the Universe and its fundamental nature using the gravitational wave sources with the network of current generation gravitational wave detectors, as shown in Fig. 3 and Fig. 4. This is not possible currently from the gravitational wave sources with EM counterparts (such as BNS and NS-BH) due to observable horizon up to a lower redshift ($z < 0.5$). As a result, only dark sirens can be used to explore the expansion history of the Universe with the currently ongoing network of gravitational wave detectors.

Along with the measurement of the expansion history, this method makes it possible to infer the gravitational wave bias parameter and its redshift dependence $b_{GW}(z)$ using the gravitational wave sources. The gravitational wave bias parameter determines the spatial distribution of the gravitational wave sources with respect to the dark matter distribution and provides an avenue to measure

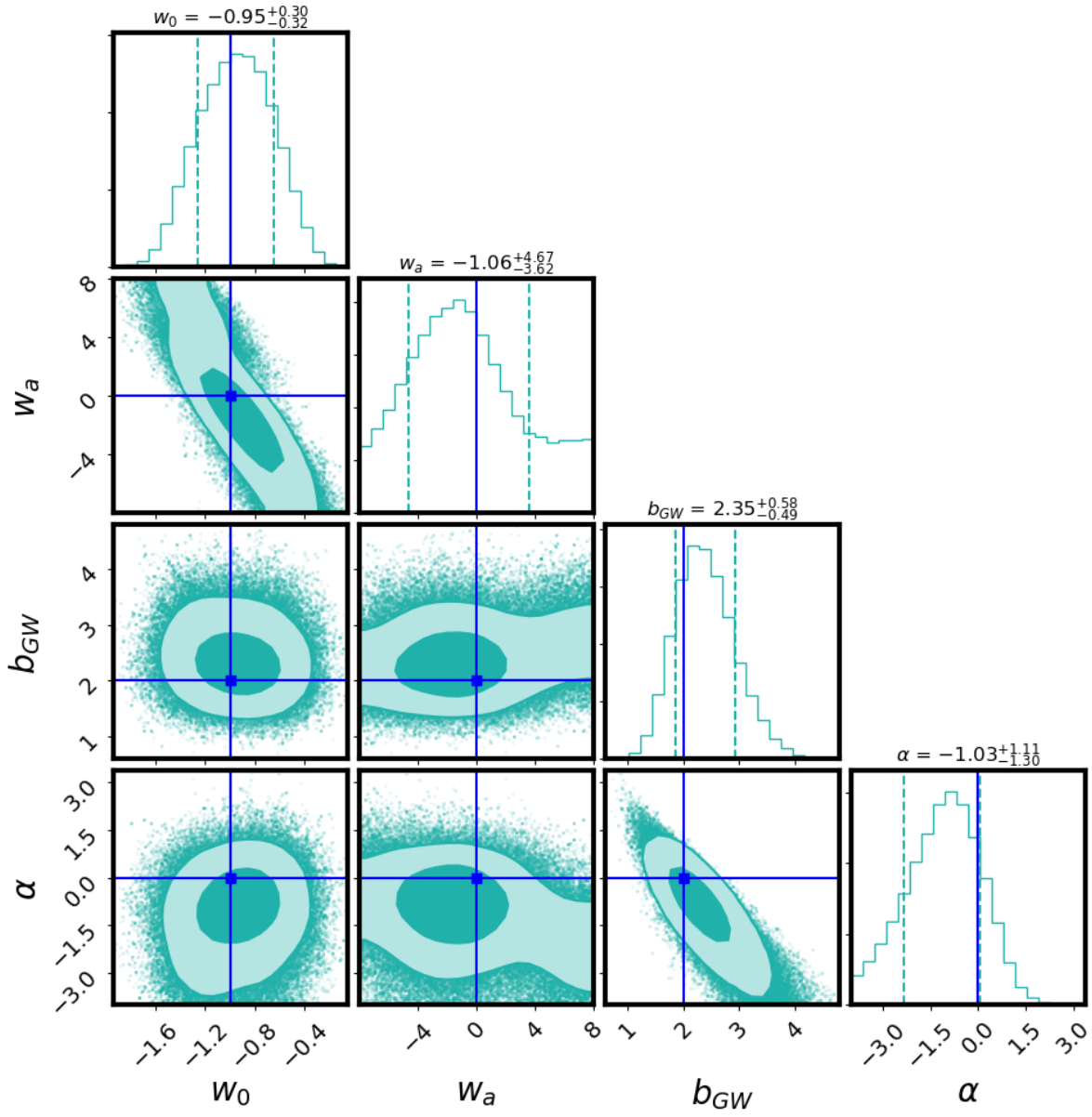

FIG. 4: We show the joint posterior of the cosmological parameters w_0 and w_a along with the nuisance parameters related to the gravitational wave bias parameter $b_{GW}(z) = b_{GW}(1+z)^{\alpha}$ for number of gravitational wave sources $N_{GW}(z) = 40$ extended up to redshift $z = 0.7$, and sky localization error $\Delta\Omega_{GW} = 10$ sq deg. The 68%, and 95% contours are shown in these plots along with the input values by the blue line. The mean value along with 1σ error-bar are mentioned in the title of the posterior distribution for all the parameters. Other cosmological parameters such as $H_0 = 70$ km/s/Mpc and $\Omega_m = 0.315$ are kept fixed for these results.

this. Using our method, we can measure the bias parameter by more than 3σ precision with only 200 BBHs distributed up to redshift of $z = 0.5$ as shown in Fig. 2. With the availability of the more gravitational wave sources, the bias parameter can be measured with higher precision and accuracy. The cross-correlation with the galaxies makes it possible to detect the bias parameters of gravitational wave sources sooner with higher statistical significance than possible from the auto-correlation [79]. The redshift dependent bias parameter is not degenerate with the cosmological parameters as shown in Fig. 2, Fig. 3, and Fig. 4, which makes it possible to reliably detect the cosmological parameters even if the gravitational wave bias parameter is currently unknown.

In the longer timescale with the operation of the next-generation gravitational wave detectors such as LISA [61], ET [62], and CE [63], we will be able to probe the expansion history of the Universe up to a much higher

redshift using the method proposed in this paper, without inferring the EM counterparts to the gravitational wave sources. So, the method proposed in this paper will help in building the observation strategy of the future gravitational wave detectors.

Finally, this method is not limited to gravitational wave sources but also applicable to any other distance tracers to infer the expansion history of the Universe using the luminosity distance – redshift relation. Our method is readily applicable to SNe samples which will be detected with photometric redshift measurement from Rubin Observatory [86], as already pointed by a previous analysis [67]. In future, this method can play a crucial role for cosmology with type-Ia SNe [104]. This method will be useful in exploring the synergy between the upcoming missions such as DES [105], Dark Energy Spectroscopic Instrument (DESI) [90], Euclid [87], SpectroPhotometer for the History of the Universe, Epoch of Reionization, and Ices Explorer (SPHEREx) [92], Nancy Grace Roman Telescope [19] [88, 89, 91]. This method is also applicable to Fast Radio Burst (FRBs) [106] to infer their redshift for which host identification will be difficult.

ACKNOWLEDGMENTS

Authors would like to thank Archisman Ghosh for carefully reviewing the manuscript and providing useful comments. S. M. also acknowledges useful discussion with Rahul Biswas, Neal Dalal, Will Farr, Archisman Ghosh, Salman Habib, Eiichiro Komatsu, Daniel M. Scolnic and Joseph Silk. This analysis was carried out at the Horizon cluster hosted by Institut d'Astrophysique de Paris. We thank Stephane Rouberol for smoothly running the Horizon cluster. SM and SMN is also supported by the research program Innovational Research Incentives Scheme (Vernieuwingsimpuls), which is financed by the Netherlands Organization for Scientific Research through the NWO VIDI Grant No. 639.042.612-Nissanke. The work of BDW is supported by the Labex ILP (reference ANR-10-LABX-63) part of the Idex SUPER, received financial state aid managed by the Agence Nationale de la Recherche, as part of the programme Investissements d'avenir under the reference ANR-11-IDEX-0004-02. The Center for Computational Astrophysics is supported by the Simons Foundation. AS acknowledges support from the NWO and the Dutch Ministry of Education, Culture and Science (OCW) (through NWO VIDI Grant No. 2019/ENW/00678104 and from the D-ITP consortium). In this analysis, we have used the following packages: Corner [107], emcee: The MCMC Hammer [108], IPython [109], Matplotlib [110], nbodykit [93], NumPy [111], and SciPy [112]. The authors would like to thank the LIGO/Virgo scientific collaboration for providing the noise curves. LIGO is funded by the U.S. National Science Foundation. Virgo is funded by the French Centre National de Recherche Scientifique (CNRS), the Italian Istituto Nazionale della Fisica Nucleare (INFN) and the Dutch Nikhef, with contributions by Polish and Hungarian institutes.

[1] E. Hubble, Proceedings of the National Academy of Science **15**, 168 (1929).
[2] S. Perlmutter et al. (Supernova Cosmology Project), Astrophys. J. **517**, 565 (1999), astro-ph/9812133.
[3] M. J. Reid, J. A. Braatz, J. J. Condon, L. J. Greenhill, C. Henkel, and K. Y. Lo, ApJ **695**, 287 (2009), 0811.4345.
[4] A. G. Riess, S. Casertano, W. Yuan, L. M. Macri, and D. Scolnic, Astrophys. J. **876**, 85 (2019), 1903.07603.
[5] Planck collaboration (Planck), Astron. Astrophys. **571**, A16 (2014), 1303.5076.
[6] L. Anderson et al. (BOSS), Mon. Not. Roy. Astron. Soc. **441**, 24 (2014), 1312.4877.
[7] E. Aubourg et al., Phys. Rev. **D92**, 123516 (2015), 1411.1074.
[8] P. Ade et al. (Planck), Astron. Astrophys. **594**, A13 (2016), 1502.01589.
[9] E. Macaulay et al. (DES), Mon. Not. Roy. Astron. Soc. **486**, 2184 (2019), 1811.02376.
[10] R. Jimenez and A. Loeb, Astrophys. J. **573**, 37 (2002), astro-ph/0106145.
[11] J. Simon, L. Verde, and R. Jimenez, Phys. Rev. D **71**, 123001 (2005), astro-ph/0412269.
[12] D. Stern, R. Jimenez, L. Verde, M. Kamionkowski, and S. Stanford, JCAP **02**, 008 (2010), 0907.3149.
[13] R. Jimenez, A. Cimatti, L. Verde, M. Moresco, and B. Wandelt, JCAP **03**, 043 (2019), 1902.07081.
[14] T. Abbott et al. (DES), Mon. Not. Roy. Astron. Soc. **480**, 3879 (2018), 1711.00403.
[15] N. Aghanim et al. (Planck) (2018), 1807.06209.
[16] K. C. Wong et al. (2019), 1907.04869.
[17] L. Verde, T. Treu, and A. Riess, in *Tensions between the Early and the Late Universe* (2019), 1907.10625.
[18] W. L. Freedman et al. (2019), 1907.05922.
[19] M. Rigault et al. (Nearby Supernova Factory) (2018), 1806.03849.
[20] C. Kochanek, Mon. Not. Roy. Astron. Soc. **493**, 1725 (2020), 1911.05083.
[21] B. F. Schutz, Nature **323**, 310 (1986).
[22] D. E. Holz and S. A. Hughes, ApJ **629**, 15 (2005), astro-ph/0504616.
[23] N. Dalal, D. E. Holz, S. A. Hughes, and B. Jain, Phys. Rev. D **74**, 063006 (2006), astro-ph/0601275.
[24] C. L. MacLeod and C. J. Hogan, Phys. Rev. D **77**, 043512 (2008), .
[25] S. Nissanke, D. E. Holz, S. A. Hughes, N. Dalal, and J. L. Sievers, ApJ **725**, 496 (2010), 0904.1017.

[19] Previouly known as Wide-Field InfraRed Survey Telescope (WFIRST)

[26] B. F. Schutz, Classical and Quantum Gravity **28**, 125023 (2011), 1102.5421.
[27] S. Nissanke, D. E. Holz, N. Dalal, S. A. Hughes, J. L. Sievers, and C. M. Hirata (2013), 1307.2638.
[28] L. Sun et al. (2020), 2005.02531.
[29] C. Messenger and J. Read, Phys. Rev. Lett. **108**, 091101 (2012), 1107.5725.
[30] W. M. Farr, M. Fishbach, J. Ye, and D. Holz, Astrophys. J. Lett. **883**, L42 (2019), 1908.09084.
[31] C. Howlett and T. M. Davis (2019), 1909.00587.
[32] S. Mukherjee, G. Lavaux, F. R. Bouchet, J. Jasche, B. D. Wandelt, S. M. Nissanke, F. Leclercq, and K. Hotokezaka (2019), 1909.08627.
[33] C. Nicolaou, O. Lahav, P. Lemos, W. Hartley, and J. Braden (2019), 1909.09609.
[34] H.-Y. Chen, M. Fishbach, and D. E. Holz, Nature **562**, 545 (2018), 1712.06531.
[35] S. M. Feeney, H. V. Peiris, A. R. Williamson, S. M. Nissanke, D. J. Mortlock, J. Alsing, and D. Scolnic, Phys. Rev. Lett. **122**, 061105 (2019), 1802.03404.
[36] R. Abbott et al. (LIGO Scientific, Virgo) (2020), 2004.08342.
[37] G. Ghirlanda et al., Science **363**, 968 (2019), 1808.00469.
[38] K. Mooley, A. Deller, O. Gottlieb, E. Nakar, G. Hallinan, S. Bourke, D. Frail, A. Horesh, A. Corsi, and K. Hotokezaka, Nature **561**, 355 (2018), 1806.09693.
[39] K. Hotokezaka, E. Nakar, O. Gottlieb, S. Nissanke, K. Masuda, G. Hallinan, K. P. Mooley, and A. Deller, Nature Astron. (2019), 1806.10596.
[40] B. P. Abbott et al. (LIGO Scientific, Virgo), Phys. Rev. Lett. **119**, 161101 (2017), 1710.05832.
[41] B. P. Abbott et al. (LIGO Scientific, Virgo, 1M2H, Dark Energy Camera GW-E, DES, DLT40, Las Cumbres Observatory, VINROUGE, MASTER), Nature **551**, 85 (2017), 1710.05835.
[42] F. Foucart, T. Hinderer, and S. Nissanke, Phys. Rev. D **98**, 081501 (2018), 1807.00011.
[43] M. W. Coughlin et al., Astrophys. J. Lett. **885**, L19 (2019), 1907.12645.
[44] I. Andreoni et al., Astrophys. J. **890**, 131 (2020), 1910.13409.
[45] B. Abbott et al. (LIGO Scientific, Virgo), Astrophys. J. Lett. **892**, L3 (2020), 2001.01761.
[46] R. Abbott et al., The Astrophysical Journal **896**, L44 (2020).
[47] M. M. Kasliwal et al. (2020), 2006.11306.
[48] D. J. Mortlock, S. M. Feeney, H. V. Peiris, A. R. Williamson, and S. M. Nissanke, Phys. Rev. D **100**, 103523 (2019), .
[49] M. J. Graham, K. E. S. Ford, B. McKernan, N. P. Ross, D. Stern, K. Burdge, M. Coughlin, S. G. Djorgovski, A. J. Drake, D. Duev, et al., Phys. Rev. Lett. **124**, 251102 (2020), .
[50] W. Del Pozzo, Phys. Rev. D **86**, 043011 (2012), 1108.1317.
[51] R. Nair, S. Bose, and T. D. Saini, Phys. Rev. D **98**, 023502 (2018), 1804.06085.
[52] R. Gray, I. M. n. Hernandez, H. Qi, A. Sur, P. R. Brady, H.-Y. Chen, W. M. Farr, M. Fishbach, J. R. Gair, A. Ghosh, et al., Phys. Rev. D **101**, 122001 (2020), .
[53] M. Fishbach et al. (LIGO Scientific, Virgo), Astrophys. J. Lett. **871**, L13 (2019), 1807.05667.
[54] B. Abbott et al. (LIGO Scientific, Virgo) (2019), 1908.06060.
[55] M. Soares-Santos et al. (DES, LIGO Scientific, Virgo), Astrophys. J. Lett. **876**, L7 (2019), 1901.01540.
[56] R. Abbott et al. (LIGO Scientific, Virgo), Astrophys. J. **896**, L44 (2020), 2006.12611.
[57] F. Acernese, M. Agathos, K. Agatsuma, D. Aisa, N. Allemandou, A. Allocca, J. Amarni, P. Astone, G. Balestri, G. Ballardin, et al., Classical and Quantum Gravity **32**, 024001 (2014), .
[58] B. P. Abbott et al., Phys. Rev. D **93**, 112004 (2016), [Addendum: Phys.Rev.D 97, 059901 (2018)], 1604.00439.
[59] T. Akutsu et al. (KAGRA), Nat. Astron. **3**, 35 (2019), 1811.08079.
[60] C. Unnikrishnan, Int. J. Mod. Phys. D **22**, 1341010 (2013), 1510.06059.
[61] P. Amaro-Seoane, H. Audley, S. Babak, J. Baker, E. Barausse, P. Bender, E. Berti, P. Binetruy, M. Born, D. Bortoluzzi, et al., arXiv e-prints arXiv:1702.00786 (2017), 1702.00786.
[62] M. Punturo et al., Class. Quant. Grav. **27**, 194002 (2010).
[63] D. Reitze et al., Bull. Am. Astron. Soc. **51**, 035 (2019), 1907.04833.
[64] L. S. Finn, Phys. Rev. Lett. **73**, 1878 (1994), .
[65] S. R. Taylor, J. R. Gair, and I. Mandel, Phys. Rev. D **85**, 023535 (2012), .
[66] M. Oguri, Phys. Rev. D **93**, 083511 (2016), .
[67] S. Mukherjee and B. D. Wandelt (2018), 1808.06615.
[68] S. Mukherjee, B. D. Wandelt, and J. Silk (2019), 1908.08951.
[69] S. Mukherjee, B. D. Wandelt, and J. Silk, Phys. Rev. D **101**, 103509 (2020), 1908.08950.
[70] P. J. E. Peebles and E. J. Groth, ApJ **196**, 1 (1975).
[71] M. Davis and P. J. E. Peebles, ApJS **34**, 425 (1977).
[72] M. Davis and P. J. E. Peebles, ApJ **267**, 465 (1983).
[73] A. J. S. Hamilton, ApJ **417**, 19 (1993).
[74] S. D. Landy and A. S. Szalay, ApJ **412**, 64 (1993).
[75] N. Kaiser, MNRAS **227**, 1 (1987).
[76] A. Hamilton, in *Ringberg Workshop on Large Scale Structure* (1997), astro-ph/9708102.
[77] S. Mukherjee and J. Silk, Mon. Not. Roy. Astron. Soc. **491**, 4690 (2020), 1912.07657.
[78] F. Calore, A. Cuoco, T. Regimbau, S. Sachdev, and P. D. Serpico (2020), 2002.02466.
[79] A. Vijaykumar, M. Saketh, S. Kumar, P. Ajith, and T. R. Choudhury (2020), 2005.01111.
[80] L. Anderson, E. Aubourg, S. Bailey, D. Bizyaev, M. Blanton, A. S. Bolton, J. Brinkmann, J. R. Brownstein, A. Burden, A. J. Cuesta, et al., MNRAS **427**, 3435 (2012), 1203.6594.
[81] V. Desjacques, D. Jeong, and F. Schmidt, Phys. Rept. **733**, 1 (2018), 1611.09787.
[82] S. Alam, M. Ata, S. Bailey, F. Beutler, D. Bizyaev, J. A. Blazek, A. S. Bolton, J. R. Brownstein, A. Burden, C.-H. Chuang, et al., MNRAS **470**, 2617 (2017), 1607.03155.
[83] T. B. Price, *LII. An essay towards solving a problem in the doctrine of chances. By the late Rev. Mr. Bayes* (cited January 1763).
[84] B. Abbott et al. (LIGO Scientific, Virgo), Phys. Rev. X **9**, 031040 (2019), 1811.12907.
[85] B. Abbott et al. (LIGO Scientific, Virgo), Astrophys. J.

Lett. **882**, L24 (2019), 1811.12940.
[86] LSST Science Collaboration, P. A. Abell, J. Allison, S. F. Anderson, J. R. Andrew, J. R. P. Angel, L. Armus, D. Arnett, S. J. Asztalos, T. S. Axelrod, et al., ArXiv e-prints (2009), 0912.0201.
[87] A. Refregier, A. Amara, T. D. Kitching, A. Rassat, R. Scaramella, J. Weller, and f. t. Euclid Imaging Consortium, ArXiv e-prints (2010), 1001.0061.
[88] J. Green, P. Schechter, C. Baltay, R. Bean, D. Bennett, R. Brown, C. Conselice, M. Donahue, X. Fan, B. S. Gaudi, et al., arXiv e-prints arXiv:1208.4012 (2012), 1208.4012.
[89] D. Spergel, N. Gehrels, J. Breckinridge, M. Donahue, A. Dressler, B. S. Gaudi, T. Greene, O. Guyon, C. Hirata, J. Kalirai, et al., arXiv e-prints arXiv:1305.5425 (2013), 1305.5425.
[90] A. Aghamousa et al. (DESI) (2016), 1611.00036.
[91] O. Dore et al. (WFIRST), ArXiv e-prints (2018), 1804.03628.
[92] O. Dore et al., arXiv (2018), 1805.05489.
[93] N. Hand, Y. Feng, F. Beutler, Y. Li, C. Modi, U. Seljak, and Z. Slepian, Astron. J. **156**, 160 (2018), 1712.05834.
[94] S. Fairhurst, Class. Quant. Grav. **28**, 105021 (2011), 1010.6192.
[95] M. L. Chan, Ph.D. thesis, Glasgow U. (2018).
[96] B. Sathyaprakash and S. Dhurandhar, Phys. Rev. D **44**, 3819 (1991).
[97] C. Cutler and E. E. Flanagan, Phys. Rev. **D49**, 2658 (1994), gr-qc/9402014.
[98] R. Balasubramanian, B. Sathyaprakash, and S. Dhurandhar, Phys. Rev. D **53**, 3033 (1996), [Erratum: Phys.Rev.D 54, 1860 (1996)], gr-qc/9508011.
[99] A. Ghosh, W. Del Pozzo, and P. Ajith, Phys. Rev. D **94**, 104070 (2016), 1505.05607.
[100] P. Ajith et al., Phys. Rev. **D77**, 104017 (2008), [Erratum: Phys. Rev.D79,129901(2009)], 0710.2335.
[101] S. W. Hawking and W. Israel, *Three hundred years of gravitation* (Cambridge University Press, 1987).
[102] E. Poisson and C. M. Will, Phys. Rev. **D52**, 848 (1995), gr-qc/9502040.
[103] M. Maggiore, *Gravitational Waves: Volume 1: Theory and Experiments*, Gravitational Waves (OUP Oxford, 2008), ISBN 9780198570745, .
[104] D. Scolnic et al. (2019), 1903.05128.
[105] D. E. S. Collaboration:, T. Abbott, F. B. Abdalla, J. Aleksic, S. Allam, A. Amara, D. Bacon, E. Balbinot, M. Banerji, K. Bechtol, et al., Monthly Notices of the Royal Astronomical Society **460**, 1270 (2016), ISSN 0035-8711, https://academic.oup.com/mnras/article-pdf/460/2/1270/8117541/stw641.pdf, .
[106] E. Petroff, J. Hessels, and D. Lorimer, Astron. Astrophys. Rev. **27**, 4 (2019), 1904.07947.
[107] D. Foreman-Mackey, The Journal of Open Source Software **24** (2016), .
[108] D. Foreman-Mackey, D. W. Hogg, D. Lang, and J. Goodman, PASP **125**, 306 (2013), 1202.3665.
[109] F. Pérez and B. E. Granger, Computing in Science and Engineering **9**, 21 (2007), ISSN 1521-9615, .
[110] J. D. Hunter, Computing In Science & Engineering **9**, 90 (2007).
[111] S. van der Walt, S. C. Colbert, and G. Varoquaux, Computing in Science and Engineering **13**, 22 (2011), 1102.1523.
[112] E. Jones, T. Oliphant, P. Peterson, et al., *SciPy: Open source scientific tools for Python* (2001–), [Online; accessed ¡today¿], .

Accurate and precision Cosmology with redshift unknown gravitational wave sources

Mukherjee, Suvodip; Wandelt, Benjamin D; Nissanke, Samaya M; Silvestri, Alessandra

01 Bruno SANCHEZ Page 1
9/7/2020 13:56

02 Bruno SANCHEZ Page 1
9/7/2020 13:57

03 Bruno SANCHEZ Page 1
9/7/2020 13:57

04 Bruno SANCHEZ Page 1
9/7/2020 13:57

05 Bruno SANCHEZ Page 1
9/7/2020 14:31

06 Bruno SANCHEZ Page 1
9/7/2020 14:33

07 Bruno SANCHEZ Page 1
9/7/2020 14:33

08 Bruno SANCHEZ Page 1
9/7/2020 14:33

09 Bruno SANCHEZ Page 1
9/7/2020 14:33

10 Bruno SANCHEZ Page 1

9/7/2020 14:29

11 Bruno SANCHEZ Page 1

9/7/2020 14:34

12 Bruno SANCHEZ Page 1

9/7/2020 14:30

13 Bruno SANCHEZ Page 1

9/7/2020 14:34

14 Bruno SANCHEZ Page 1

9/7/2020 14:35

15 Bruno SANCHEZ Page 1

9/7/2020 14:38

16 Bruno SANCHEZ Page 2

9/7/2020 14:39

17 Bruno SANCHEZ Page 2

9/7/2020 14:38

18 Bruno SANCHEZ Page 2

9/7/2020 14:38

19 Bruno SANCHEZ Page 2

9/7/2020 14:39

20 Bruno SANCHEZ Page 2

9/7/2020 14:39

21 Bruno SANCHEZ Page 3

9/7/2020 15:44

22 Bruno SANCHEZ Page 3

9/7/2020 14:44

23 Bruno SANCHEZ Page 3

9/7/2020 15:24

24 Bruno SANCHEZ Page 3

9/7/2020 15:44

25 Bruno SANCHEZ Page 3

9/7/2020 15:46

26 Bruno SANCHEZ Page 3

9/7/2020 15:23

27 Bruno SANCHEZ Page 3

9/7/2020 15:46

28 Bruno SANCHEZ Page 3

9/7/2020 15:24

29 Bruno SANCHEZ Page 3

9/7/2020 15:46

30 Bruno SANCHEZ Page 3

9/7/2020 15:46

31 Bruno SANCHEZ Page 3

9/7/2020 15:46

32 Bruno SANCHEZ Page 3

9/7/2020 15:24

33 Bruno SANCHEZ Page 3

9/7/2020 15:43

34 Bruno SANCHEZ Page 3

9/7/2020 15:43

35 Bruno SANCHEZ Page 3

9/7/2020 15:47

36 Bruno SANCHEZ Page 3

9/7/2020 15:44

37 Bruno SANCHEZ Page 3

9/7/2020 15:48

38 Bruno SANCHEZ Page 3

9/7/2020 15:48

39 Bruno SANCHEZ Page 4

9/7/2020 15:54

40 Bruno SANCHEZ Page 4

9/7/2020 15:52

41 Bruno SANCHEZ Page 4

9/7/2020 15:49

42 Bruno SANCHEZ Page 4

9/7/2020 15:53

43 Bruno SANCHEZ Page 4

9/7/2020 15:49

44 Bruno SANCHEZ Page 4

9/7/2020 16:03

45 Bruno SANCHEZ Page 4

9/7/2020 17:22

46 Bruno SANCHEZ Page 4

9/7/2020 17:22

47 Bruno SANCHEZ Page 4

9/7/2020 15:56

48 Bruno SANCHEZ Page 4

9/7/2020 15:56

49 Bruno SANCHEZ Page 5

9/7/2020 17:11

50 Bruno SANCHEZ Page 5

9/7/2020 17:11

51 Bruno SANCHEZ Page 5

9/7/2020 17:12

52 Bruno SANCHEZ Page 5

9/7/2020 17:12

53 Bruno SANCHEZ Page 5

9/7/2020 17:11

54 Bruno SANCHEZ Page 5

9/7/2020 17:12

55 Bruno SANCHEZ Page 5

9/7/2020 17:12

56 Bruno SANCHEZ Page 5

9/7/2020 17:12

57 Bruno SANCHEZ Page 5

9/7/2020 17:12

58 Bruno SANCHEZ Page 5

9/7/2020 17:12

59 Bruno SANCHEZ Page 5

9/7/2020 15:56

60 Bruno SANCHEZ Page 5

9/7/2020 17:13

61 Bruno SANCHEZ Page 5

9/7/2020 17:14

62 Bruno SANCHEZ Page 5

9/7/2020 17:17

63 Bruno SANCHEZ Page 5

9/7/2020 17:17

64 Bruno SANCHEZ Page 5

9/7/2020 17:11

65 Bruno SANCHEZ Page 5

9/7/2020 17:24

66 Bruno SANCHEZ Page 5

9/7/2020 17:24

67 Bruno SANCHEZ Page 7

9/7/2020 16:07

68 Bruno SANCHEZ Page 7

9/7/2020 16:07

69 Bruno SANCHEZ Page 7

9/7/2020 16:08

70 Bruno SANCHEZ Page 7

9/7/2020 16:08

71 Bruno SANCHEZ Page 7

9/7/2020 16:08

72 Bruno SANCHEZ Page 7

9/7/2020 16:08

73 Bruno SANCHEZ Page 7

9/7/2020 16:09

74 Bruno SANCHEZ Page 7

9/7/2020 16:09

75 Bruno SANCHEZ Page 7

9/7/2020 16:09

76 Bruno SANCHEZ Page 7

9/7/2020 16:10

77 Bruno SANCHEZ Page 7

9/7/2020 16:10

78 Bruno SANCHEZ Page 7

9/7/2020 16:10

79 Bruno SANCHEZ Page 8

9/7/2020 16:10

80 Bruno SANCHEZ Page 8

9/7/2020 16:11

81 Bruno SANCHEZ Page 8

9/7/2020 16:11

82 Bruno SANCHEZ Page 8

9/7/2020 16:11

83 Bruno SANCHEZ Page 8

9/7/2020 16:12

84 Bruno SANCHEZ Page 9

9/7/2020 16:12

85 Bruno SANCHEZ Page 9

9/7/2020 16:13

86 Bruno SANCHEZ Page 9

9/7/2020 16:12

87 Bruno SANCHEZ Page 10

9/7/2020 16:13

88 Bruno SANCHEZ Page 10

9/7/2020 16:13

89 Bruno SANCHEZ Page 10

9/7/2020 16:20

90 Bruno SANCHEZ Page 10

9/7/2020 16:14

91 Bruno SANCHEZ Page 10

9/7/2020 16:14

92 Bruno SANCHEZ Page 10

9/7/2020 16:16

93 Bruno SANCHEZ Page 10

9/7/2020 16:16

94 Bruno SANCHEZ Page 10

9/7/2020 16:17

95 Bruno SANCHEZ Page 10

9/7/2020 16:17

96 Bruno SANCHEZ Page 10

9/7/2020 16:19

97 Bruno SANCHEZ Page 11

9/7/2020 16:15